FACULTEIT GENEESKUNDE EN GEZONDHEIDSWETENSCHAPPEN

Study on the effects of cold atmospheric plasma on murine colon cancer cells

Brit Vancoppenolle
Student number: 01806041
Isolde Van Wesemael
Student number: 01808148

Supervisors: Prof. Dr. Wim Ceelen, Prof. Dr. Olivier De Wever, Prof. Dr. Ir. Nathalie De Geyter
Counsellor: Dr. Anton Nikiforov, Dr. Sarah Cosyns, Sam Ernst

Master's thesis submitted in the context of obtaining the degree of Master of Medicine in Medicine
Academic year 2022-2023

UNIVERSITEIT GENT

Date
17/11/2022



Isolde Van Wesemael Brit Vancoppenolle Prof. Dr. Wim Ceelen

Preface

When we were assigned our thesis topic, we found ourselves in uncharted waters. Our master's thesis covers several aspects we knew little about beforehand, such as physics and biomedicine. We had no knowledge of the research ahead of us, but were eager to delve into it. After four years of studying, where the focus was mainly on the theoretical aspect of medicine, we were looking forward to getting in touch with the research side as well. Only thanks to all the help we received, we can now proudly present this work.

First of all, we would like to thank **Prof. Dr. Wim Ceelen** and **Dr. Sarah Cosyns** immensely for the space they gave us to get creative with the experiments ourselves, for their support when needed, for their guidance and expertise and for their continued patience when the experiments did not always go as planned.

Second, we would like to thank **Prof. Dr. Olivier De Wever** for the opportunity to work in the LECR lab and for helping to form an initial idea regarding the possible experiments. We are very grateful to all laboratory staff and PhD students for their guidance and support in the lab. Special thanks go to **Sam Ernst** who taught us all the necessary laboratory techniques and helped us plan, re-plan and conduct our experiments. Thank you for always being there for us throughout the process and giving so much time to guide our master's thesis.

We would also like to thank **Prof. Dr. Ir. Nathalie De Geyter** for allowing us to work in the physics lab and familiarising us with the possibilities of the physical aspects of the experiments. Furthermore, we would particularly like to thank **Dr. Anton Nikiforov** for sharing his knowledge and experience on the topic, for helping us set up and plan the experiments and for answering our endless questions and requests to check our work.

Finally, we would like to thank all the people around us, especially my sisters and Loïc, for their moral support in going through the medical course and writing the master's thesis. Thank you for the many pep talks, endless support and for proofreading this entire work with a critical eye. We are very grateful to our parents for giving us the opportunity to go to university and for always being there for us.

Contents

Terms and definitions

ASCII	a 7-bit character code where every single bit represents a unique character
AvaSoft	a software package developed to control all Avantes spectrometers and a wide range of accessories
DAMP	Damage-associated molecular patterns are molecules within cells associated with the innate immune response. They are released by damaged or dying cells due to trauma or an infection by a pathogen.
DMEM	Dulbecco's Modified Eagle Medium
FBS	fetal bovine serum, the most widely used serum-supplement for the in vitro cell culture of eukaryotic cells
FWHM	full width at half maximum
GFP-Luc	The jellyfish green fluorescent protein (GFP) and the firefly luciferase (Luc) are two commonly used molecular reporters that can be detected noninvasively in living cells to monitor cell viability.
Line ratio method	a method in which the intensity ratio of emission lines is related to electron temperature and electron density
LOM	light optical microscopy
Lorentzian Distribution	Also known as the Cauchy distribution, is an example of a distribution which has no mean, variance or higher moments defined. Its mode and median are well defined. Compared to the normal distribution, it has a higher peak and lower tails

MAPK/ERK	The MAPK/ERK pathway is a chain of proteins in the cell that communicates a signal from a receptor on the surface of the cell to the DNA in de nucleus of the same cell.
MassiveOES	a software, developed specifically for the analysis of optical emission spectra of plasma discharges, that fits simulations to measured data
MTS assay	A methyltransferase assay is used to assess cell proliferation, cell viability and cytotoxicity.
NIST	an atomic spectra database
N_2(C-B)	transition of N_2 from level C to level B
$PBSD^-$	Phosphate-buffered saline is used to disengage attached and clumped cells.
Peak-to-peak difference	the difference between the maximum voltage amplitude and the minimum voltage amplitude
RNS	reactive nitrogen species
ROS	reactive oxygen species
RONS	reactive oxygen and nitrogen species
Gaussian distribution	Gaussian functions are widely used in statistics to describe normal distributions. The graph is a characteristic symmetric "bell curve" shape.
Technical control	an experiment conducted in the same settings as a previous experiment to increase the reliability of the results by excluding the influence of variables

Abstract

The aim of this study was to identify the properties of a CAP device and its effects on cell death, specifically in a murine colorectal cancer cell line. To obtain this, physical experiments concerning gas temperature, electron temperature and current were carried out. In addition, the effect of CAP on the surface temperature of an aluminium plate, on the pH and on the conductivity of medium and NaCl after irradiation was studied. These parameters provided information on the ideal situation for irradiating cancer cells in an aluminium plate.

After obtaining these results, it was found that the best conditions were met when the nozzle of the J-plasma device was positioned at 10 mm from the liquid surface and a maximum of 16 W was set. The murine colorectal cancer cell lines CT26 and MC38 were thus irradiated at 10 mm with a power of 8 W or 16 W for 30 s or 120 s with 2 technical controls and 3 controls each not irradiated. Cell death was analysed using MTS-assay and flow cytometry with live-death staining.

MC38 and CT26 cells from the plastic well plate underwent MTS assay 48 and 72 hours after plasma treatment, respectively, to determine indirect and delayed cell death. This showed that pretty much all cells died after treatment, while the untreated cells continued to grow undisturbed. Cells treated in an aluminium well plate were stained with propidium iodide and passed through a flow cytometer to have an idea of direct and instant cell death. This showed that for the MC38 cells irradiation at (10 mm, 8 W, 120 s) resulted in the most cell death.

These results show that CAP causes direct cell death in murine colon cancer cell lines on the one hand, but also indirect cell death on the other hand. A higher applied power doesn't lead to more cell death, on the contrary, results show that there is less immediate cell death at 16 Was opposed to 8 W. Radiation duration, on the other hand, does affect cell death. The longer irradiation is used, the more cell death is observed. These results are at odds with the observations from the physics lab, where irradiation time had no effect on the observed values. The biggest factor in changing the values was rather the applied power.

Nederlandstalig abstract

Het doel van deze studie was het identificeren van de eigenschappen van een CAP-toestel en de effecten ervan op celdood, specifiek in een murine colorectale kankercellijn. Hiertoe werden fysische experimenten uitgevoerd met betrekking tot de gastemperatuur, de elektronentemperatuur en de stroomsterkte. Bovendien werd het effect van CAP op de oppervlaktetemperatuur van een aluminiumplaat, op de pH en op de geleidbaarheid van medium en NaCl na bestraling bestudeerd. Deze parameters gaven informatie over de ideale situatie voor het bestralen van kankercellen in een aluminium plaat.

Na het verkrijgen van deze resultaten bleek dat de beste omstandigheden werden bereikt wanneer de tip van het J-plasma toestel op 10 mm van het vloeistofoppervlak werd geplaatst en een maximum van 16 W werd ingesteld. De muriene colorectale kankercellijnen CT26 en MC38 werden aldus bestraald op 10 mm met een vermogen van 8 W of 16 W gedurende 30 s of 120 s met telkens 2 technische controles en 3 niet-bestraalde controles. De celdood werd geanalyseerd met behulp van MTS-assay en flowcytometrie met live-death-kleuring.

MC38- en CT26-cellen uit de plastic wellplaat ondergingen respectievelijk 48 en 72 uur na de plasmabehandeling een MTS-test om de indirecte en vertraagde celdood te bepalen. Hieruit bleek dat vrijwel alle cellen na de behandeling stierven, terwijl de onbehandelde cellen ongestoord bleven groeien. De in een plaat met aluminium putjes behandelde cellen werden gekleurd met propidiumjodide en door een flowcytometer gevoerd om een idee te krijgen van de directe en onmiddellijke celdood. Hieruit bleek dat voor de MC38-cellen bestraling bij (10 mm, 8 W, 120 s) de meeste celdood tot gevolg had.

Deze resultaten tonen aan dat CAP enerzijds directe celdood veroorzaakt bij muriene darmkankercellijnen, maar anderzijds ook indirecte celdood. Een hoger toegepast vermogen leidt niet tot meer celdood, integendeel, de resultaten tonen aan dat er minder directe celdood is bij 16 W in tegenstelling tot 8 W. De bestralingsduur daarentegen is wel van invloed op de celdood. Hoe langer er wordt bestraald, hoe meer celdood wordt waargenomen. Deze resultaten staan haaks op de waarnemingen uit het fysicalabo, waar de bestralingstijd geen effect had op de waargenomen waarden. De grootste factor bij het veranderen van de waarden was veeleer het toegepaste vermogen.

1. Introduction

In 2020, the WHO estimated that there were more than 1.9 million new cases of colorectal cancers (CRC), accounting for 935 000 deaths and one-tenth of all cancer cases (1). Colorectal cancer is increasing in prevalence over the last decade, with a lifelong chance of development of 5% (2). In 2019, it was the third and second most frequent cancer in respectively men and women in Belgium (3). Due to the rising prevalence, additional attention was paid to the development of new treatment options. The current treatment options consist of local endoscopic resection, surgical treatment, radiotherapy for rectal cancers, systemic treatment, local ablative therapies for metastases and palliative chemotherapy, depending on the characteristics of the cancer in question (4). Together with earlier diagnosis, because of screening programs, this has led to an increase in overall survival (5).

Still, metastatic colorectal cancer (mCRC) accounts for a large amount of the lasting mortality, with a 1 year survival of 70-75%, 3 year survival of 30-35% and fewer than 20% of the patients surviving beyond 5 years from diagnosis. mCRC occurs in 20% of colorectal cancers at presentation and 25% of the patients develop metastasis during and after treatment of the localized disease. The most common sites of metastasis include lymph nodes, liver, lung, and peritoneum (6). One in five patients with colorectal cancer develops peritoneal minimal residual disease after surgical resection, and about one in seven patients develops peritoneal carcinomatosis (7). Established peritoneal carcinomatosis (PC) from CRC is much less responsive to systemic therapy and causes considerable morbidity in affected patients. Developing a new treatment option for peritoneal metastasis can considerately decrease patient mortality (8).

One of the developing new techniques used in oncology is cold atmospheric plasma (CAP). CAP is a promising technique used in a variety of medical and biological applications. CAP is shown to have an inhibitory effect on cancer cells in vitro and in vivo in several types of cancers. More specifically, plasma treatment is shown to have an effect on colon cancer cells, such as inhibition of cell proliferation and induction of cell death (9). One of the main underlying mechanisms is the generation of ROS and RNS (10-13), but further research is needed to fully understand the process of cancer cell death and the impact of the plasma properties.

1.1 What is cold atmospheric plasma?

The term ‘plasma’ refers to the fourth state of matter (14-17). It is achieved by ionization of gas particles creating an equal amount of positive and negative charged particles (10, 12, 14, 16-21). Because of their composition, plasmas are chemically active and electrically conductive (18, 22).

There are two large groups of plasma systems namely thermal and non-thermal systems. Of these systems, the non-thermal systems are, because of their characteristics, more compatible with the biomedical world. These features include high excitation selectivity and energy efficiency in combination with low plasma temperatures. An advancement was made when laboratories worked on developing a system that could generate plasma under atmospheric pressure instead of under vacuum conditions, which would make the devices more convenient to use. As a result of these recent developments, CAP has a low gas temperature, a high reactive chemical species density and more easily than before, control over the plasma dynamics. Therefore, numerous biomedical applications of CAPs emerged (18, 22-24).

Over the last few years, more and more applications of CAPs have emerged across various biomedical disciplines (13, 15, 22, 25). Fridman et al. mentions uses of plasmas for sterilization (living tissue and non-living objects), blood coagulation, wound healing and tissue regeneration, cancer treatment, treatment of skin diseases, treatment of corneal infections and others (15).

There are several types of plasma sources which can be divided into different categories regarding their excitation mode: direct current (DC) and low frequency discharges, plasmas ignited by radiofrequency (RF) waves and microwave (MW) discharges (18). Each of these plasma sources have their own characteristics and their own advantages and disadvantages.

Depending on the manner of ionization, the circumstances in which the plasma is generated (vacuum or atmospheric pressure), the excitation mode and the device itself, the properties of the plasma change (18).

In this research, the J-Plasma portion of the Bovie Ultimate High Frequency Electrosurgical Generator device was used. Helium gas particles were ionized by applying non-thermal energy, specifically a radio frequency (RF) voltage, to reach the plasma state. This process was carried out under atmospheric pressure.

1.2 Physical aspects

The electric field in the J-Plasma device supplies energy to the helium gas, ionizes it and generates electrons. The generated electrons in turn collide with the neutral species (= atoms, molecules) present in the gas. As a result, the majority of the supplied electrical energy is used for the production of energetic electrons and excited or ionized species, instead of heating the gas (23). Two types of collisions are possible: elastic and inelastic. Elastic collisions only increase the kinetic energy of the neutral species, but do not change their internal energy, whereas inelastic collisions also increase the internal energy of the neutral species. This process can be attributed to the fact that, if the electron energy is high enough, a collision will result in a change in the electron structure of the neutral species, resulting in the formation of excited species, free radicals and ions. Most of these excited species have a short lifetime and fall back to the ground state by emitting photons or initiating chemical processes.

Depending on the type of energy supply and the amount of energy added to the plasma, its properties change. Based on electron density and electron temperature, plasma can be divided into several categories, where one of the most important differences is between an LTE (local thermal equilibrium) and a non-LTE plasma. LTE plasmas are thermal plasmas with the following characteristics: $T_e = T_h \approx$ 10 000's K. Non-LTE plasmas are cold plasmas where $T_e \approx$ 10 000 - 100 000 K and $T_h \approx$ 300 - 1000 K. The non-LTE plasmas can thus be described by a two temperature model: an electron temperature (T_e) and a heavy particles temperature (T_h). The plasma temperature (or gas temperature) is fixed by T_h. When LTE is reached, the plasma can be operating in the arc mode. The higher the deviation from LTE, the higher the difference between T_e and T_h is (18).

The device used in this research, as stated before, is a radiofrequency discharge, more specifically an APPJ (atmospheric pressure plasma jet). Radiofrequency driven APPJs provide high densities of ROS and radicals at low gas temperatures (26). A voltage is applied between two electrodes resulting in the ionized gas leaving through the nozzle of the plasma jet. Due to the low power discharge, transition into the arc state is prevented (18).

1.3 Mechanisms of cancer cell death

Recent research found that CAP has the ability to cause apoptosis in certain cancer cells and stop/slow down proliferation while not delivering permanent harm to normal cells. The apoptosis could be attributed to the activation of caspases (27, 28). CAP can selectively harm and kill cancerous cells. In addition, synergistic effects of CAP on chemotherapy and

immunotherapy have been described (15, 19, 20). This effect was observed in pancreatic cancer cells, where application of TTP (tissue tolerable plasma, Argon as carrier gas) leads to a decrease in cell viability due to apoptotic and non-apoptotic cell death. In the top layers of the tumours a decrease in Ki67+ proliferating cells was noticed. In prostate cancer cells the same effects on apoptosis and proliferation have been observed (17, 27).

CAP induces immunogenic cell death (ICD) in melanoma cells by increasing the expression of surface-exposed calreticulin (CRT), the most critical DAMP in ICD. The same effect was observed in CT26 colorectal tumours with additionally an increased recruitment of CD11+ and CD45+ immune cells. Furthermore, CAP stimulates the recruitment of macrophages and cytotoxic T cells. In breast cancer cells, a similar increase in CRT was observed, but in addition, the molecules HSP70, HSP90, MHC-I, ATP and interferons, known to be involved in ICD, also increased (16, 21, 28).

One of the major contributors in ICD is the generation of reactive oxygen and nitrogen species ($^{\bullet}OH$, O_2, O_2^-, $^{\bullet}NO$, O/O_3, $ONOO^-$, H_2O_2, NO_2^-, NO_3^-). RONS regulate intracellular and intercellular biochemical pathways inducing chemical and physical changes in cells. For instance, activating tumour suppressor proteins and kinases, suppressing the oncogenic PI3K/AKT pathway leading to initiation of cancer cell death. This pathway is also associated with metastasis in some tumours. Other research showed that plasma suppresses cell invasion and migration, indicating that CAP could play a role in preventing metastasis (12, 29).

Moreover, RONS can interact with the cell DNA. In order to accomplish these effects, they have to penetrate the surface of the treated cells. After RONS generation, they are encountered with a first barrier: the cell membrane. This leads to either a reaction with or a crossing of the membrane. Interactions between RONS and the cell membrane result in lipid peroxidation, increasing the membrane permeability. Together with the electrical field of the J-Plasma, this facilitates the plasma delivery of RONS within the tissue to millimetre depths. The penetration of plasma effects is further established through cell-to-cell communication, where surface cells, directly exposed to the plasma, transmit effects to subsurface cells.

As a consequence of a different cell membrane composition between cancer cells and healthy cells, the RONS will penetrate better into cancer cells. On the one hand, this can be attributed to a higher concentration of cholesterol in healthy cell membranes, reducing the ingress of RONS. Otherwise, the higher number of aquaporin on cancer cells membranes lead to a more important flow of RONS in cancer cells (16, 21, 28, 30, 31). A supplementary effect on cancer

cells can be attributed to the counteraction of hypoxia by oxygenating the tissue. This results in a reduced resistance of cancer cells to radiation and cytotoxic drugs, while also leading to increased apoptosis, as the oxidative stress exceeds the cell survival limit more easily in cancer cells.

RONS also play an important role in the apoptotic pathway. They induce cancer cell death through activation of four MAPK pathways (ERK1/2, JNK, p38 and ERK5). JNK and p38 also increase the expression of the p53 tumour suppressor gene. The ERK pathway regulates proliferation, differentiation, cycle regulation, apoptosis, tissue formation, tumour proliferation and invasion/metastasis. Regulating this pathway can be a key factor in inhibiting tumour growth. Furthermore, RONS play a part in the process of autophagy, ferroptosis and pyroptosis resulting in even more cancer cell death (12).

In colorectal cancer cells the following effects of CAP were observed: generation of RONS, decrease in cell viability, suppression of cell invasion and migration, increased apoptotic behaviour by affecting kinase signalling pathways p38, JNK and ERK and an increase in β-catenin (29).

The aim of this research is to map out safe standard settings for using the plasma device in medical settings and the effects of CAP delivered by the J-Plasma device on the viability of murine colorectal cancer cells in vitro.

2. Materials and methods

This chapter discusses the materials and methods used in the research. The design and research methods will be described, along with its justification.

The aim of these experiments is to identify the properties and effect on cancer cells of the J-Plasma device. Mapping out these properties could lead to a better understanding of the optimal conditions in which the device should be used in real life settings. Observing the effects on cancer cells could support the current findings in literature and result in a better insight in the underlying mechanisms in cancer cell death due to the application of cold atmospheric plasma.

First, the characteristics of the J-Plasma device were tested to determine the optimal settings for the treatment of cancer cells. The focus of this research is on cold atmospheric plasma that results in apoptosis of cancer cells. Under certain conditions, the plasma will change into an arc, leading to coagulation of tissue. Therefore, it is interesting to find out under which conditions the arc state was formed. To this end, experiments were conducted to determine the surface temperature, gas temperature and electron temperature, as these provide more information on the state of the plasma.

Additionally, the discharge current was measured, since this parameter also gives information about whether the arc state was established or not. Furthermore, the legal exposure of the human body to a current must not exceed 20mA, preventing possible permanent damage.
Eventually this resulted in a few possible treatment scenarios. Cells were cultured until the amount of cells was sufficient for the experiments. For these, treatment time, power of the J-Plasma device and distance between the nozzle of the plasma and the surface of the treated cells were adjusted to analyse their influence on cell death. Ultimately, viability of the cancer cells was observed.

Further on, the effects of the plasma on pH and conductivity in the medium, used to culture the cells, and in physiological water (0.9% NaCl) were examined. The formation of new molecules and ions caused by the treatment may affect the pH and conductivity. If the plasma has an influence on the pH in the culture medium, it becomes difficult to distinguish what is causing the cancer cell death, since a change in pH can also lead to apoptosis. As a result, the observed apoptosis would not be able to be attributed with 100% certainty to the plasma factors alone.

Finally, an experiment with biomembranes (BioBrain^{R}) was carried out to try and simulate more human-like conditions and determine whether the J-Plasma device is capable of damaging a synthetic epithelium.

2.1 Standard settings of the Bovie Medical J-plasma device

The J-plasma device used for the experiments was operated with a helium gas flow of 4 L/min and a pulse cycle of 80%. The power settings can be varied by changing the percentage of power applied, with the maximum power equal to 40 W.

2.2 Thermal activity on an aluminium plate

To determine the effect of a plasma treatment on the surface temperature, an aluminium plate was treated with the J-Plasma Jet, with the nozzle set at different distances (1 mm, 2.5 mm, 5 mm and 10 mm). The power settings were 8 W, 16 W and 32 W with a treatment time of 10 s, 30 s, 60 s, 120 s and 240 s. The maximum temperature of the aluminium plate was observed using a Fluke TiS45 thermal imager. A picture was taken with the Fluke camera at the end of each treatment.

2.3 Gas and electron temperature

To measure the gas temperature, an Avantes 3648 spectrometer with a wavelenght detection range of 350-390 nm was used. For the electron temperature determination, an Avantes 2048 spectrometer with a wider wavelength detection range of 250-770 nm was used. The 3648 spectrometer has a smaller wavelength range but a higher resolution of 50 pm, whereas the 2048 has a wavelength wider range but a lower resolution of 1 nm. Because of these characteristics, the 3648 spectrometer is better suited to measure the gas temperature while the 2048 spectrometer is more applicable for the electron temperature measurements using the line ratio method. The data were obtained using AvaSoft software.

An aluminium plate was treated with the J-plasma Jet, with the nozzle set at different distances (1 mm, 2.5 mm, 5 mm and 10 mm). The power settings were 8 W, 16 W and 32 W. Since time-averaged values were obtained using AvaSoft, the treatment time as well as the exposure time

do not affect the results. During the treatment, the signal was captured, via the spectrometer using AvaSoft software.

2.3.1 Optical emission spectroscopy

Spectroscopy is a collective name for scientific techniques that allow substances to be examined on the basis of their electromagnetic spectrum. Optical emission spectroscopy is a non-invasive diagnostic technique to analyse plasma parameters. An emission spectrometer collects the light emitted by the plasma itself. Here, one of the basic underlying processes is the collision of electrons with atoms/molecules causing excited species generation. Electrons do not stay in excited states for a very long time. They soon return to their ground states, emitting a photon with the same energy as the one that was absorbed.

This emitted photon corresponds with a line in the optical emission spectrum characterized by a specific wavelength and intensity. The central wavelength of line emission is given by the photon energy corresponding to the energy gap of the transition from the excited to the ground state. The line intensity depends only on the population density of the excited level which, in turn, depends strongly on the plasma parameters and emission probability of the transition. Each element has its own fingerprint of lines. The elements of focus in this research are N molecules and He atoms. Additionally, OH radicals were also examined (32).

2.3.2 Gas temperature

While using the 3648 spectrometer, the focus was on the wavelength region 373-381 nm where three nitrogen peaks attributed to the N_2(C-B) transition are located. These peaks were used instead of the OH peak at 337 nm, because of the interference with lines caused by the ionization of aluminium. The spectra obtained by the 3648 spectrometer were converted to an ASCII code (.txt) and then converted to excel (.csv). In order to be able to use MassiveOES, the original code needed to be changed from Dutch to English. The commas were transformed into points and the semicolons were transformed into commas. In MassiveOES, simulation of the N_2(C-B) band was done, the Slit fn Gaussian FWHM and the Lorentzian FWHM were checked off and the value of the Lorentzian function was set to 0.013 as defined by the specifications of the used spectrometer. As no calibration was used for the wavelength correction, there was a 1 nm difference between the experimental peaks and the theoretical values. Therefore, the X-axes were linearized and shifted to compensate for the wavelength shift.

The gas temperature (assumed to be equal to the heavy particle temperature) can be obtained from precise measurements of the line profile, in particular the line width. The gas temperature

was calculated by fitting the simulated spectrum (N_2(C-B)) to the spectra obtained under different conditions considering T_h as a variable parameter.

2.3.3 Electron temperature

While using the 2048 spectrometer, the focus was on the peaks located at 492, 438.79 and 667.81 nm where three helium peaks are located. To calculate the electron temperature the line ratio method was used with the following formula:

$$\ln\frac{I_1}{I_2}\times\frac{A_2}{A_1}\times\frac{g_2}{g_1}\times\frac{\lambda_1}{\lambda_2}=-\frac{(E_1-E_2)}{kT_e}$$

I= intensity

A = Einstein coefficients

g = statistical weight of the transition

λ = wavelength

E = energy

k = Boltzmann constant

T_e = electron temperature

By using the measured wavelength and intensity, the electron temperature was obtained. The other parameters were retrieved from the NIST database.

2.4 Current

To measure the discharge current, a Wavesurfer 3104z 1 GHz oscilloscope was used. The pulse cycle of the J-plasma device was set on 80%. Within the pulse cycle, the device should be 20% on and 80% off. The settings of the device were confirmed based on the detection of the current waveform.

The total discharge current was obtained by measuring the peak-to-peak difference. Afterwards, this number was multiplied by 0.20, taking into account the plasma is switched on for only 20% of the time. The time off was acquired by looking at the length of the period in between two pulses (= baseline). The time on corresponds to the length of 1 pulse cycle. These parameters were measured with the nozzle set at a distance of 1 mm, 2.5 mm, 5 mm, 10 mm and a variable power of 8 W, 16 W and 32W.

2.5 Cultivating cells

Murine colon adenocarcinoma (MC38GL and CT26GL) were grown in DMEM, high glucose (Thermo Fisher Scientific, 41965039) with 10% heat inactivated FBS. Penicillin and streptomycin 1-2% were added to the medium. The cells were maintained in an incubator at 37°C and 5% CO_2.

To thaw the cells, warm medium (37°C) was added dropwise to the vial with frozen cells and freezing medium using a pipette. The obtained solution/suspension of warm medium, freezing medium and cells were transferred to the centrifuge tube. When all the cells were thawed, the vial was rinsed twice with the warm medium. Then the tube was centrifuged at 200 g for 5 min. After removing the supernatant with a pasteur pipette, 1 ml of medium was added. The cell suspension was divided over 2 tissue culture flasks and medium was added to obtain ⅕ and ⅘ dilutions.

Afterwards, the cells were cultured for 2-4 days, until they reached a confluence of approximately 80%. To harvest the cells, they were washed with PBSD- and trypsinized. Then the cells were again divided over tissue culture flasks and incubated. This process was repeated until the necessary amount of cells was obtained.

To count the cells, the cell suspension of one falcon was transported into a centrifuge tube and centrifuged (200 g, 5 min). After that, the cell pellet was resuspended in medium and diluted in a trypan blue solution (ratio ½). The amount of cells was observed with an automatic cell counter on the one hand and counted manually on the other hand, both based on the trypan blue assay. The average of the two was considered as the total number of cells per 1 ml.

2.6 Treatment of cells

500 µl of suspension, containing medium and 30 000 cells of either the MC38 or CT26 cell line, was transferred into each well of a 24 aluminium and 24 plastic well plate. The MC38 and CT26 cells in the plastic well plates were incubated for respectively 48 and 72 hours to allow the cells to adhere. In contrast, the cells in the aluminium plate were treated in suspension immediately after translocation because of the potential toxicity of the aluminium on the cells. The cells were then treated with the J-Plasma jet, with the nozzle set at 10 mm above the liquid surface. The power settings were 8 W or 16 W with a treatment time of 30 s or 120 s. Three wells were not treated to serve as controls. For each condition, 3 wells were treated with the same settings to obtain 2 technical controls for each setup. Specifically, well A1, B1 and C1

were irradiated at 8 W for 30 s. A2, B2 and C2 at 8 W for 120 s. A3, B3 and C3 at 16 W for 30 s and A4, B4 and C4 at 16 W for 120 s. A5, B5 and C5 served as control.

2.6.1 Cell viability

Cell viability was analysed using an MTS assay on the one hand and life death staining followed by flow cytometry on the other hand at 0, 48 or 72 hours after treatment, depending on the confluence of the cells and whether they were treated in an aluminium well plate or a plastic well plate. The MC38 cells in plastic wells were analysed 48 hours after treatment due to their faster cell growth, while the CT26 cells in plastic wells were examined 72 hours after treatment and the cells in the aluminium wells were studied the day itself.

2.6.2 MTS assay

An MTS assay is a method to evaluate the amount of cells in a well plate. The MTS solution is a negatively charged tetrazolium reagent and needs to be incubated for four hours together with the cells to be converted into a coloured substrate. The dying cells will very rapidly lose the ability of converting the MTS solution to its coloured substrate. After incubation, the signals can be read by a plate reader. Depending on the amount of viable cells, the signal will be higher or lower. Eventually, the background can be subtracted.

In these experiments the MTS assay was performed on the cells incubated and treated in the plastic well plates respectively 48 h and 72 h after treatment for MC38 and CT26, due to their difference in growth rate (33).

2.6.3 Flow cytometry

For flow cytometry, the cells must first be stained, after which the cells are passed through the flow cytometer in a single cell suspension with a buffer. The specific flow aligns the cells, eventually causing them to pass through the system one by one. Using a laser and a detector, the flow cytometer detects each cell with its specific characteristics individually.

In this experiment, the cells treated in the aluminium plate underwent life-death staining with PI (propidium iodide). After this, the PI in the cells is excited by a 561 nm laser in the flow cytometer. When PI returns to its former state, it emits a fluorescent signal. This signal is then detected by the detector of the flow cytometer. Dead cells absorb PI better into their DNA than live ones because their cell membrane is interrupted, allowing PI to enter the cell nucleus more easily. As a result, the dead cells emit a stronger signal. This makes it possible to determine the amount of live and dead cells after treatment. The observed cell lines were also GFP-Luc

positive, but this will not interfere with the excitation of PI because GFP-Luc is only excited by a 488 nm laser.

In addition, the flow cytometer also records the scattered light. Here, a distinction can be made between forward scatter, which is used to determine cell size, and side scatter, which indicates the amount of cell granularity. The larger the cells, the more forward scatter. Increasing granularity, caused by cell death, increases the amount of lateral scatter. This results in two different cell populations, living cells and dead cells (34).

2.6.4 Analysis of the results

After flow cytometry results were obtained, the gating strategy shown in Figure S2 was applied in FlowJo, the software to analyse flow cytometry results. First, debris due to cell death was excluded and then single cells were selected. The latter because during the flow of cells through flow cytometry, cells may pass in pairs rather than as single cells and this disturbs the scattered light. Later, the cell counts were converted into percentages to improve comparability between groups. After this, these percentages were included in a dataset in SPSS. The predetermined test to perform the further analysis is the One-way ANOVA. To apply this test, the data must be sorted by group and the Levene's test must yield a non-significant result.

2.7 pH and conductivity

To evaluate the effect of the J-plasma device on pH and conductivity, 1 ml medium (DMEM) and 1 ml NaCl (0.9%) were exposed to the plasma jet for 60 s with the power set at 8 W, 16 W and 32 W. The distance between the outlet of the plasma device and the liquid differed between 1 mm, 2.5 mm, 5 mm and 10 mm. Before measuring the pH and conductivity with a Mettler Toledo device, 2.5 ml of distilled water was added to ensure that the tip of the device was sufficiently submerged in the liquid. This dilution was later taken into account.

2.8 Biomembranes

Before exposure, the biomembranes were coated with a 6% NaCl solution. They were then treated with the J-plasma jet, with the nozzle set at either 1 mm or 10 mm. The power settings were 8 W, 16 W and 32 W with a treatment time of 60 s. The maximum temperature of the aluminium plate with the biomembranes was observed using a Fluke TiS45 thermal imager. The damage was visualized under a LOM.

3. Results

This chapter will discuss the results obtained in the experiments. First of all, the surface, electron and gas temperature together with the observed current, conductivity and pH changes provide information on the optimal settings for treatment of cancer cells. Afterwards, the effect of exposing the cancer cells to the J-plasma device on cancer cell proliferation and death will be analysed.

3.1 Thermal activity on an aluminium plate

The surface temperature was observed during exposure of an aluminium plate to the J-plasma device. *Figure 1* gives an overview of the results obtained. As expected, the exposure time has no major influence on the surface temperature, since most of the points are located near the median temperature of a fixed condition. The temperature quickly reaches a saturation point because there is power feed from the plasma and power dissipation from the aluminium plate. Increasing the applied power results in adding more energy, making the temperature higher. There is a large difference in surface temperature depending on the distance. As the distance decreases and the applied power increases, the plasma moves closer to the arc state. This could explain why high temperatures are observed at short distances. The only conditions resulting in acceptable temperatures for the treatment of cancer cells are (10 mm, 8 W), (10 mm, 16 W) and (5 mm, 8 W).

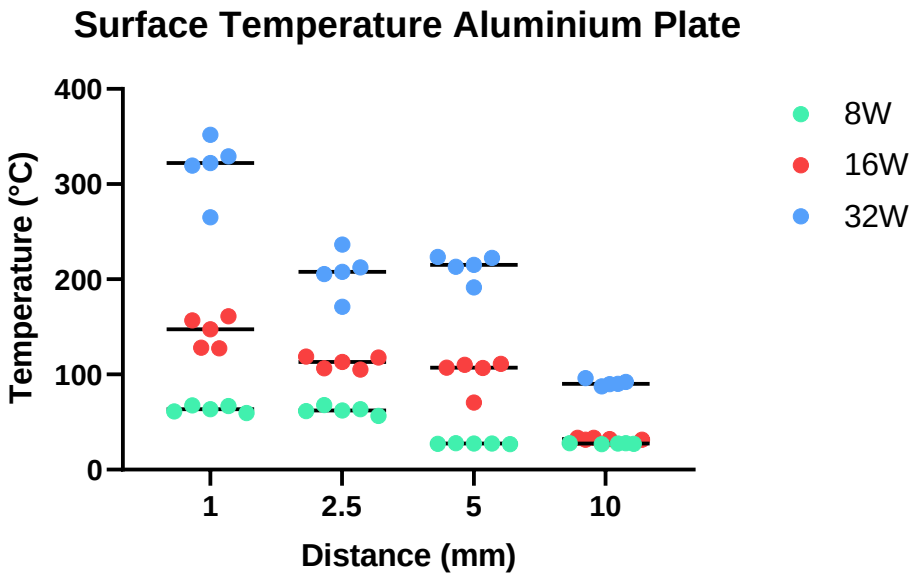

Figure 1: Surface temperature of an aluminium plate after exposure to CAP. *The x-axis represents the distance from the nozzle of the J-plasma to the surface of the aluminium plate.*

In the y-axis the observed temperature can be found. The colour code illustrates the amount of Watt. Each individual point corresponds to a specific treatment time, either 10, 30, 60, 120 or 240 seconds.

3.2 Gas and electron temperature

3.2.1 Gas temperature

As mentioned above, the gas temperature was obtained by the use of a spectrometer. As shown in *Figure 2* the gas temperature rises with increasing power. This can be explained by the fact that the plasma gets closer to the arc state under these conditions. From the time the plasma is in arc mode, T_h (gas temperature) is expected to be within the limits of 10 000-100 000 K, while T_h in the non-LTE state (jet) should be between 300-1000 K, as mentioned above. Here, the plasma is never fully in the arc state, but at high powers, the plasma is further away from the pure jet state.

There is a small trend of decreasing gas temperature with increasing distance. Again, this can be explained by the fact that the plasma gets closer to the arc state at low distances. For some unknown reason, the gas temperature was lower at (1 mm 8/16 W) than at 2.5 mm and highest at (10 mm, 32 W). This could be a measurement error caused by the chosen spectrum of N2 molecules, which is less reliable than the spectrum of OH radicals. As mentioned above, peaks caused by the ionization of aluminium interfered with the lines of OH radicals, resulting in an unreliable interpretation of this spectrum.

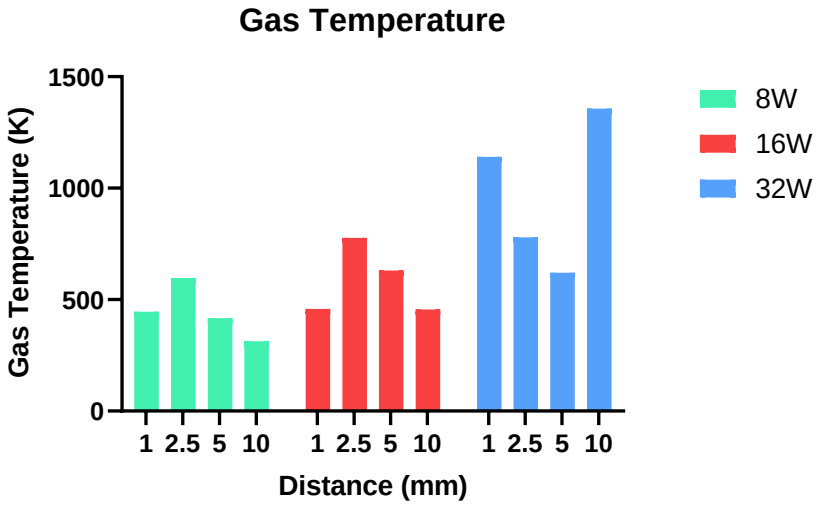

Figure 2: Gas temperature while treating an aluminium plate with CAP. *The x-axis represents the distance from the nozzle of the J-plasma to the surface of the aluminium plate. In the y-axis the observed gas temperature can be found. The colour code illustrates the*

amount of Watt. Each bar represents one measured value of the gas temperature at specific conditions.

The treatment was carried out using an atmospheric pressure plasma jet (APPJ) utilizing a radiofrequency discharge. Gas temperatures below 600 K are expected (18). The conditions under which the jet state is reached meet these expectations. As one gets closer to the arc state, the gas temperatures exceed 600 K. The publication by Tendero et al. does not mention the arc state.

3.2.2 Electron temperature

The electron temperature follows the expected pattern, but isn't always in the right order of magnitude. As previously mentioned, plasmas in non-LTE have a Te between 10 000-100 000 K, whereas LTE plasmas have a Te around 10 000 K. As shown in Figure 3 the closer the plasma gets to the arc state, the lower the electron temperature is. Tendero et al. assumes the electron temperature of an APJJ to be between 10 000 and 20 000 K (18). The cause of the observed discrepancy could be due to the fact that the temperature of the plasma is really high which could lead to too much background noise to get the most reliable results.

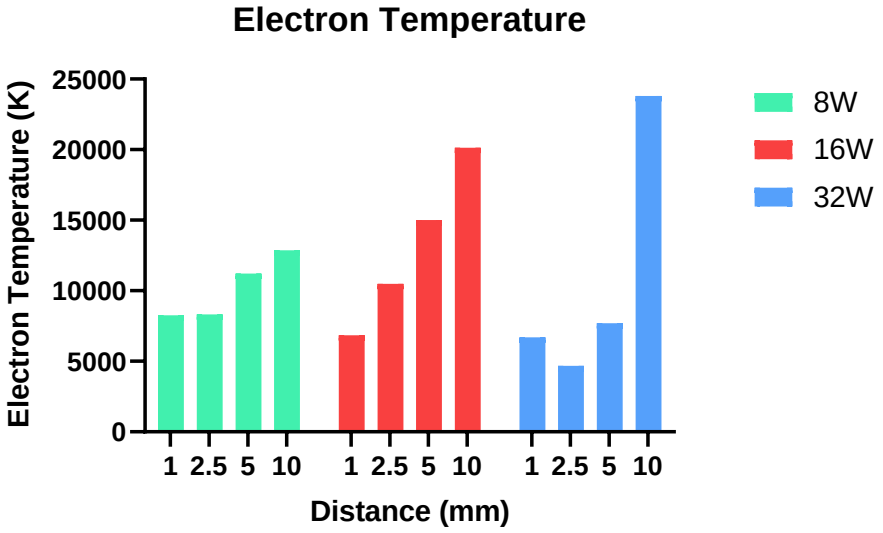

Figure 3: Electron temperature while treating an aluminium plate with CAP. *The x-axis represents the distance from the nozzle of the J-plasma to the surface of the aluminium plate. In the y-axis the observed electron temperature can be found. The colour code illustrates the amount of Watt. Each bar represents one measured value of the electron temperature at specific conditions.*

3.3 Current

The legal exposure of the human body to a current not resulting in permanent damage should not exceed 20 mA. The only experimental setting where this condition is met, is at (10 mm 8 W) resulting in a discharge current of 0.0028 A. Here, the plasma works like a jet, meaning there is no direct coupling between the plasma and the aluminium plate, so only capacitive current flows through the system. The capacitive current is expected to be low, hence the measured result. In all other situations, the current is too high, which is probably due to approaching the arc state, because there not only the capacitive current but also the resistive current, which is dominant, has to be taken into account.

3.4 pH

Starting at a pH of 7.79 and 7.76 for respectively NaCl and medium, the pH decreases as the applied power increases, but this change is more prominent in NaCl than in medium. This could be attributed to the fact that the medium contains a buffer. By exposing NaCl and medium to the plasma, reactions take place possibly resulting in the formation of $Al(OH)_3$ changing the pH. Since the pH changes in the medium are relatively subtle it's not expected to have any impact on cell death. Therefore, it doesn't have to be taken into account as a factor in cell death as a result of exposure to the plasma jet.

Furthermore, a change in colour of the medium was noticed. On the one hand, this could be caused by a decrease in pH, on the other hand, when the plasma turns into an arc, the observed beam could immediately denature proteins in the medium resulting in a change of colour. The fast denaturation could be due to many free radicals. This could be a plausible explanation since the colour changes were only observed in conditions where plasma was closer to the arc state.

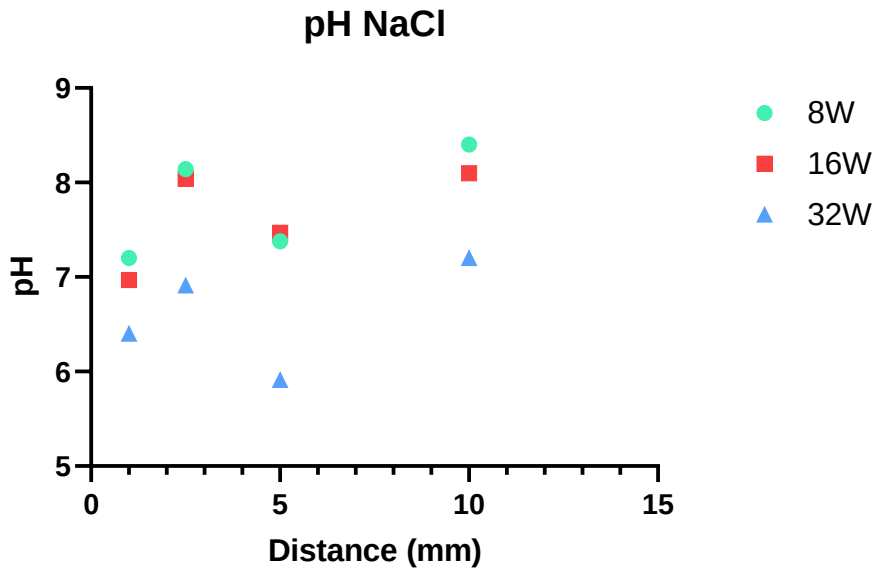

Figure 4: pH of an NaCl solution after exposure to J-plasma (starting point pH = 7.79). *The x-axis represents the distance from the nozzle of the J-plasma to the surface of the NaCl solution. In the y-axis the measured pH can be found. The colour code illustrates the amount of Watt.*

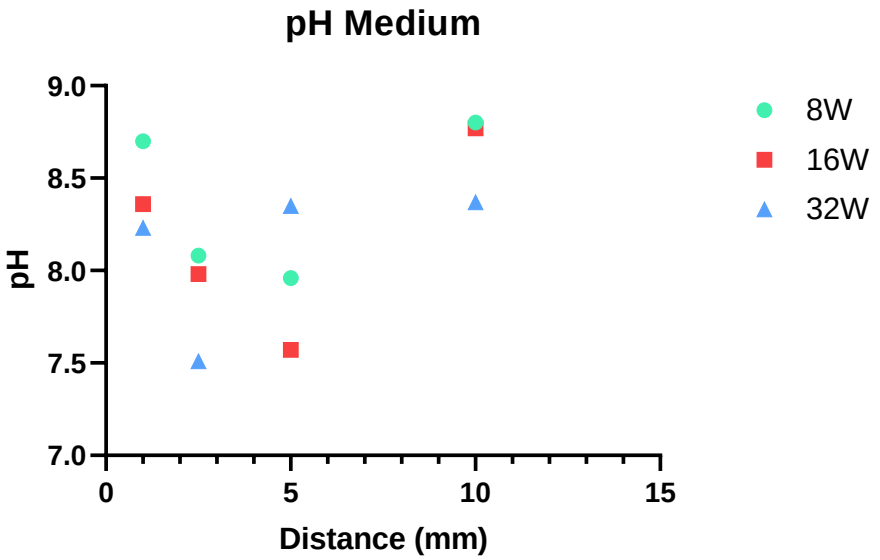

Figure 5: pH of cell culture medium after exposure to J-plasma (starting point pH = 7.76). *The x-axis represents the distance from the nozzle of the J-plasma to the surface of the medium. In the y-axis the measured pH can be found. The colour code illustrates the amount of Watt.*

3.5 Conductivity

Starting at 14.60 mS/cm, the conductivity of the NaCl solution decreased unexpectedly and to a high extent. It was hypothesized that conductivity would increase due to the formation of NO_3^- and NO_2^- as a result of interaction between plasma and air. One explanation could be that the following reaction took place: NaCl → 3NaOH + Al → $Al(OH)_3$ where Cl_2 dissolves in air and $Al(OH)_3$ is insoluble. This results in a loss of ions, which explains the decrease in conductivity. Starting at 4.52 mS/cm, treatment with the J-plasma didn't have a great influence on the conductivity of the medium, therefore it doesn't have to be taken into account as a factor in cell death as a result of exposure to the plasma jet. At (10 mm, 16 W), there is a decrease in the conductivity of the medium that cannot be explained by any theory. Therefore, this is assumed to be an experimental error.

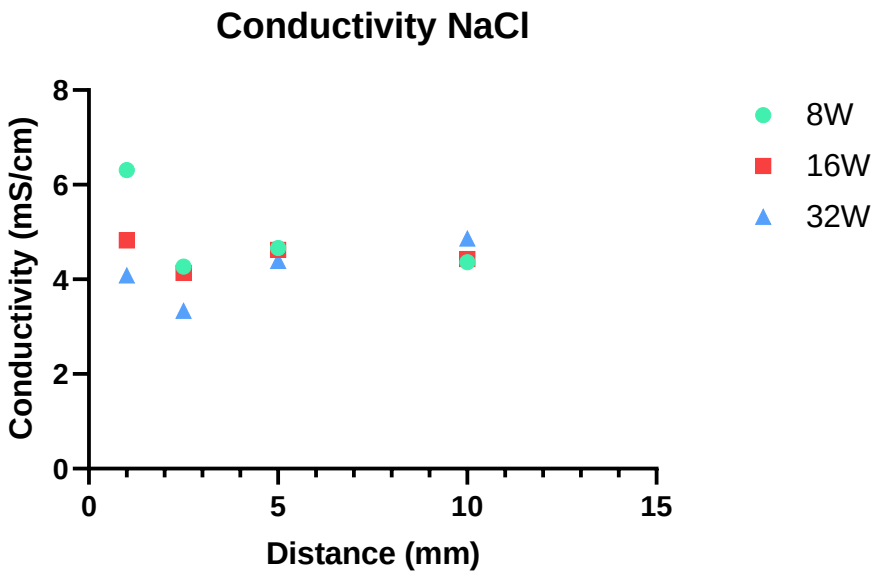

Figure 6: Conductivity of an NaCl solution after exposure to J-plasma (starting point conductivity = 14.60 mS/cm). *The x-axis represents the distance from the nozzle of the J-plasma to the surface of the NaCl solution. In the y-axis the measured conductivity can be found. The colour code illustrates the amount of Watt.*

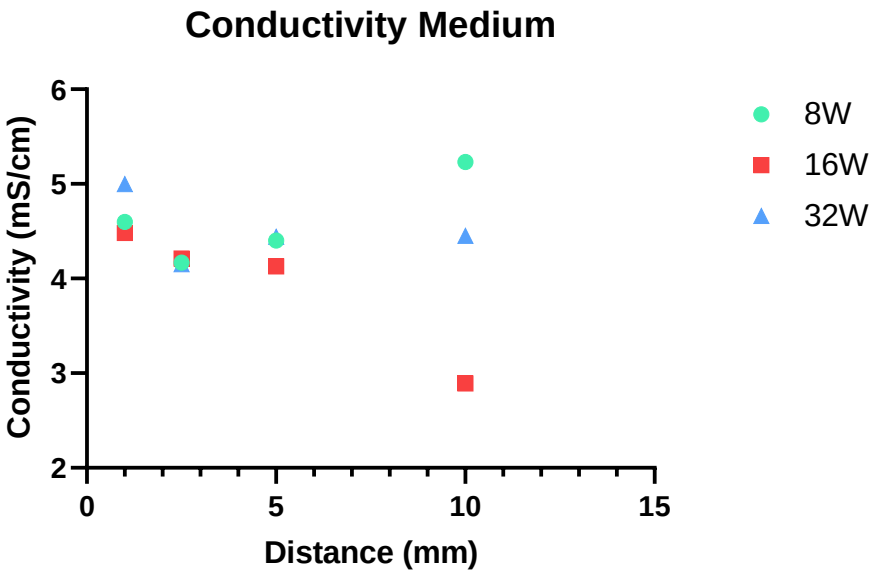

Figure 7: Conductivity of cell culture medium after exposure to J-plasma (starting point conductivity = 4.52 mS/cm). *The x-axis represents the distance from the nozzle of the J-plasma to the surface of the medium. In the y-axis the measured conductivity can be found. The colour code illustrates the amount of Watt.*

3.6 Biomembranes

The observed damage to the biomembranes is larger with increasing power and at a closer distance. Nevertheless, the damage obtained on biomembranes cannot be extrapolated to the expected damage on skin. The microscopic image of (10 mm, 8 W) was more difficult to interpret because there was already previous damage to the biomembrane that was not caused by exposure to the J-plasma device.

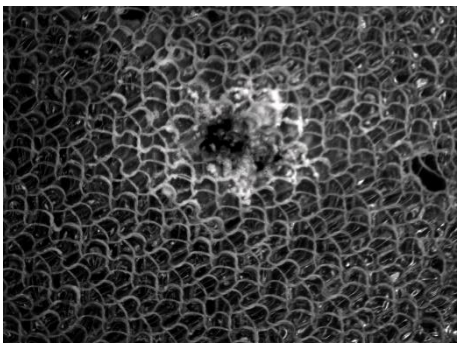

Image 1: Microscopic view of a biomembrane after treatment with J-plasma at (1 mm, 32 W)

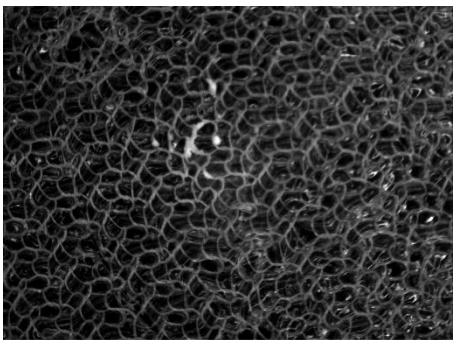

Image 2: Microscopic view of a biomembrane after treatment with J-plasma at (10 mm 16 W)

3.7 Treatment of cells

3.7.1 MTS assay

MTS assay was performed on the treated cells from the MC38 and CT26 cell lines. In addition, an MTS assay was also performed on pure medium without cells to have an idea of the background. This came out at 0.29. If this number is subtracted from the results obtained for MC38 and CT26, only the staining obtained by the cells remains and there is no interference with the effect of medium.

3.7.1.1 MC38

As shown in *Figure 8* the situations with 120 s of irradiation seem to cause more cell death than 30 s of treatment. Nevertheless, if the background of 0.29 is subtracted there is almost no signal left indicating that all cells died 48 h post treatment with CAP. D3 and D4 show that untreated cells continued their growth undisturbed.

	1	2	3	4
A	0,326	0,282	0,307	0,289
B	0,308	0,289	0,307	0,281
C	0,334	0,287	0,311	0,286
D	OVRFLW	OVRFLW	3,837	3,409

Figure 8: Results from the plate reader of MC38 cells after MTS assay. *A1 = B1 = C1 = 10 mm, 8 W, 30 s, A2 = B2 = C2 = 10 mm, 8 W, 120 s, A3 = B3 = C3 = 10 mm, 16 W, 30 s, A4 = B4 = C4 = 10 mm, 16 W, 120 s, D1-4 = control.*

3.7.1.2 CT26

The difference between the different configurations of treatment is smaller here than with MC38. There is almost no discrepancy to be noticed between the various setups. The same result as for MC38 is observed, namely that, when you factor in the background, almost all cells died 72 h post treatment. D1-4 again show that untreated cells continue their growth undisturbed. The signal is lower than that of MC38 because the cells of the CT26 cell line have a slower growth rate.

	1	2	3	4
A	0,243	0,244	0,228	0,231
B	0,245	0,258	0,254	0,235
C	0,235	0,257	0,274	0,306
D	1,243	1,236	1,493	1,4

Figure 9: Results from the plate reader of CT26 cells after MTS assay. *A1 = B1 = C1 = 10 mm, 8 W, 30 s, A2 = B2 = C2 = 10 mm, 8 W, 120 s, A3 = B3 = C3 = 10 mm, 16 W, 30 s, A4 = B4 = C4 = 10 mm, 16 W, 120 s, D1-4 = control.*

3.7.2 Flow cytometry

As mentioned above, treated cells in the aluminium well plate underwent live-dead staining immediately after treatment, followed by flow cytometry. The percentages of dead and live cells were obtained through the FowJo software for all the different treatments for both MC38 and CT26. The percentages of dead cells were then used to analyse and compare the different treatments to determine whether a particular treatment condition resulted in significantly more cell death. In SPSS, the tests for homogeneity of variances (Levene's test) had a non-significant result. Thus, this meant that all conditions were met to perform a one-way ANOVA.

3.7.2.1 MC38

The one-way ANOVA showed a significant result ($p<0.001$) for the MC38 cell line. This means that at least two of the population averages, where a population are the wells of the same equally treated cell line (e.g. A1, B1 and C1), are significantly different. To investigate this further, the post hoc test Tuckey was applied.

As shown in *Figure S4* the averages of the different groups were compared. The only groups that consistently showed significant results compared to the other groups were group 2 and group 5. Group 2 were the wells in which the cells were treated at a distance of 10 mm, with a power of 8 W and a treatment time of 120 s. Group 5 contained the wells that served as controls. No significant differences were found between the other groups.

Since group 5 is the control and the control was significantly different ($p<0.05$) from all other groups, we can conclude that there was a significant difference between the cells that were treated and the cells that were not treated. Also, the mean of dead cells of group 5 was lower than that of the other groups (*figure 10*). This means that the treatment has a significant effect

on the amount of dead cells and thus the conclusion is that all tested treatments lead to cell death to a greater or lesser extent.

It was expected that the higher the wattage, the higher the cell death. But contrary to expectations, beside group 5, group 2 was the only group that differed significantly ($p<0.05$) from all groups. Moreover, the mean of dead cells of group 2 was higher than the mean of the other groups (*figure 10*). Concluding from these findings, group 2 had the greatest difference in dead cells, meaning that treatment at a distance of 10 mm, with a power of 8 W and a treatment time of 120 s caused the greatest amount of cell death.

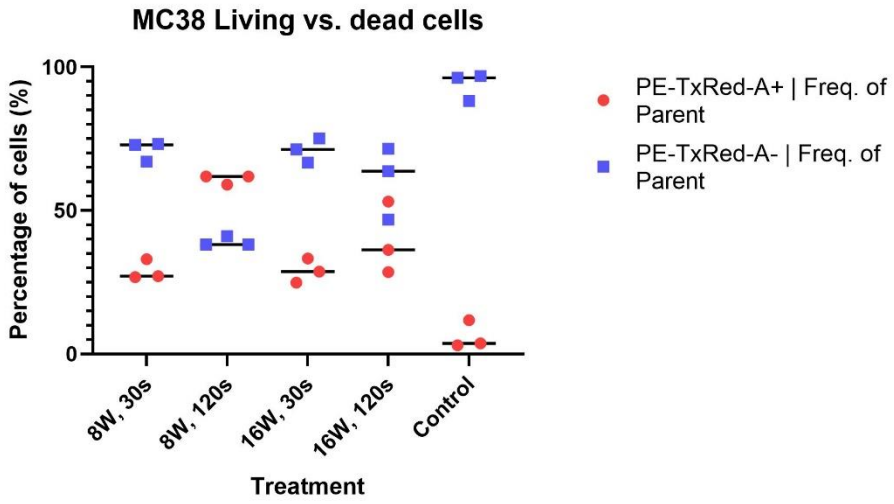

Figure 10: Percentage of MC38 cells after treatment. *The x-axis shows the treatment state. The y-axis shows the percentage of cells. The colour code distinguishes between dead and live cells. Dead cells are red and live cells are blue.*

3.7.2.2 CT26

In contrast to the results on the MC38 cell line, the one-way ANOVA showed a non-significant result ($p>0.001$). This means we could not statistically demonstrate a significant difference between the treatments.

In general, the same trends seem to emerge as for the MC38 cell line. The group that underwent treatment at a distance of 10 mm, with a power of 8 W and a treatment time of 120 s (group 2) generally had more dead cells than the other groups. Similarly, the control group (group 5) generally had the fewest dead cells (*figure 11*). However, the same conclusions cannot be drawn as for the MC38 cell lines. The difference in significance between MC38 and

CT26 could be due to the smaller amount of cells counted by the flow cytometer, which may have led to a less reliable percentage of dead and live cells. Moreover, only three samples were taken in each group, which again might have led to less reliable results.

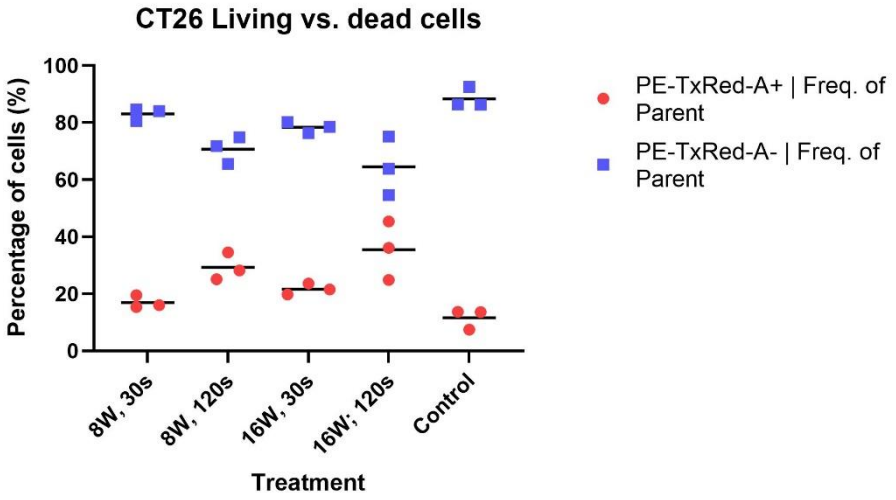

Figure 11: Percentage of CT26 cells after treatment. *The x-axis shows the treatment state. The y-axis shows the percentage of cells. The colour code distinguishes between dead and live cells. Dead cells are red and live cells are blue.*

4. Discussion

This chapter critically reflects on the experiments conducted and the results obtained. Furthermore, recommendations are made regarding future research.

4.1 Implementation of the experiments

4.1.1 Physical experiments

While analysing the surface temperature on the aluminium plate, the fluke camera used to make the measurements also became hot. Since the heat given off by the camera itself was greater than the temperature created by the reaction between plasma and aluminium, the camera focused on its own temperature rather than on the point where the plasma reached the aluminium plate at low temperatures. Therefore, the focus point was manually set to the collision area between the beam and the plate, leading to a less accurate analysis at low temperatures.

The discharge current was studied while the J-plasma irradiated the surface of an aluminium plate, producing a high value when there was coupling between the plasma beam and the aluminium plate, which is the case in arc-like situations. This setting produced only one human-safe situation. Since the treatment of the cells was performed with a layer of 500µl medium and cells above the aluminium bottom, it would have been more useful to analyse the current with the nozzle of the plasma set at a certain distance above the same layer of medium. It is expected that in this situation there would have been less coupling between the plasma jet and the aluminium plate, as it was visually observed that the arc state was approached more slowly during the cell treatment than during the observation of the current on the aluminium surface. This would have resulted in less resistive current, leading to lower current in general and more situations safe for human settings.

During the investigation of pH and conductivity, the observed values kept fluctuating when the probe was placed in the respective liquid. Therefore, the average value of all displayed numbers was recorded as an observation. As a result, the measurements of this device may not be 100% reliable. However, the overall trend was assumed to be in the right order of magnitude.

4.1.2 Experiments on cells

Unlike the plastic well plate, the aluminium plate for treatment of cells was not sterile. This wasn't assumed to be a problem since the cells were only in there for 3 hours and they didn't have to attach to the bottom, as the cells were treated in suspension. The sterility of the plate is especially important in situations where the cells are in it for long periods of time to avoid bacterial contamination.

Cells were treated either suspended in medium or attached to the bottom of the wells with a medium layer of 500 µl above. It was assumed that indirect cell death was caused by generation of ROS and RNS in the medium. In contrast, the Bovie Medical plasma Jet is used in current practice to treat peritoneal metastases. Here, cancer cells are irradiated directly without the intervention of medium. It is difficult to say whether the experimental situation with medium is comparable to the clinical situation with cancer cells and their intracellular matrix and peritoneal fluid. Therefore, it would be interesting to conduct future experiments in which the medium is removed after treatment and replaced with fresh medium to neutralise the effect of the treated medium on the attached cells.

4.2 Analysis of the findings

4.2.1 Physical experiments

The experiments were conducted on an aluminium plate to determine the optimal settings for cell treatment. It was later decided that additional experiments would also be carried out in plastic well plates. Therefore, it would have been convenient to have the same data on the effects of the J-plasma on plastic, since the results from aluminium cannot be extrapolated to plastic. First, this was something that was noticed during the treatment of cells. arc-like discharges observed above aluminium were absent above plastic for exactly the same settings, suggesting that the arc mode arises faster in aluminium, possibly due to the easy coupling of plasma and aluminium. Moreover, the surface temperature of a material is highly dependent on its heat capacity, leading to completely different results depending on the material.

The observation of gas and electron temperature required a laptop to analyse the spectra obtained. During this study, there were times when the plasma beam interfered with the laptop's electromagnetic waves, preventing the computer programme from being used. This

was only observed in situations where the plasma was closer to the arc state. This is something that should definitely be avoided in OR settings.

After plasma treatment, it was observed that there was direct cell death by the J-plasma and indirect cell death possibly caused by the generation of ROS and RNS. Therefore, it would also be useful to analyse pH and conductivity 48-72 hours after plasma irradiation to observe the possible effects of ROS and RNS on these parameters in medium and NaCl.

4.2.2 Experiments on cells

After the treatment on aluminium, direct cell death was observed by the use of flow cytometry analysis. The effect of the treated aluminium plate on the cells is not known. There is a chance that aluminium may be ionised during treatment which is potentially toxic to the cells and leads to cell death. Therefore, when analysing cell death, it should be kept in mind that the cell death was possibly partly caused by aluminium itself and not 100% by the plasma. For this reason, a plastic well plate was used as a control.

This flow cytometry analysis was performed on each well of the 24 well plate with a specific experimental set-up containing 30 000 cells each. For more accurate results, experiments with about 250 000 cells/well should be performed, but the general trend of the results was considered correct. 10 000 of the 30 000 cells were analysed each time to get a quick overview of the cell population in each well. In the case of the CT26 cell line, a difficulty was observed in achieving the set 10 000 cells. This is probably due to the fact that there were fewer than 30 000 cells in the wells of this cell line. This could possibly be explained by an error when transferring the cells to the 24 well plate or counting the cells. Nevertheless, the overall trend seemed to be in the right order of magnitude, but more cells are needed for more reliable flow cytometry analysis.

For cell transfer, a cell suspension was placed in a centrifuge, creating a cell palate at the bottom of a centrifuge tube. Sometimes these palates were quite small and thus a bit more unstable. Manipulation of these palates to dissolve them in new medium could have led to loss of cells.

When counting cells, there was often a small difference between the automatic and the manual cell counter. Therefore, the average of the two was used to determine the number of cells in a falcon. In the CT26 cell line, cells sometimes appeared clustered under the microscope,

making it difficult to determine how many live cells a cluster contained. This could possibly have led to a cell counting error, resulting in less than 30 000 cells being transferred per well.

Moreover, flow cytometry showed that (10 mm, 8 W, 120 s) was the condition that resulted in the most cell death. Contrary to expectations, a higher power did not lead to more cell death; on the contrary, 8 W caused more cell death than 16 W in almost all controls. One possible explanation could be that a higher power causes deeper penetration of the plasma beam into the medium, bringing the focal point of the plasma to the bottom of the plate rather than directly on the cells, leading to less direct cell death. This is just a theory, but it would be interesting for future research to analyse what happens to the plasma beam in the medium itself. Furthermore, it is also difficult to say whether the cells were directly and evenly treated by the plasma jet or whether some cells, which are in the focal point of the plasma jet, are more affected.

4.3 Future research

4.3.1 Extrapolation to human and clinical conditions

The surface temperature experiment in this study was conducted on an aluminium surface. The heat capacity of aluminium differs greatly from the heat capacity of the peritoneum of the human body. This means that the findings on temperature cannot be properly extrapolated to the expected surface temperature on peritoneum. In general, the findings concerning aluminium are specific to this material, as plasma interaction with aluminium is a determining factor in the formation of the arc mode. It is assumed that these interactions are material-specific and therefore it would be interesting to perform these physical experiments on peritoneum or cadaver skin.

In this study, the setup was based on predetermined fixed conditions, as opposed to manual use in practice. Moreover, the distance used in clinical settings is rather of the order of centimetres, while most studies use distances of the order of millimetres. This means that the plasma in the studies is often closer to the arc state, as shown in the results, and has more characteristics of coagulation. This has a negative effect on extrapolability to the clinic.

To try to mimic more human-like conditions, biomembranes were used to get a better view of possible plasma exposure damage. At the same time, the surface temperature was monitored with a Fluke camera. However, this setup is still not comparable to the human situation, as the aluminium is directly below the biomembrane, which means that its properties are still closer

to those of aluminium, so coupling can still occur between the plasma and the plate, which could lead to the formation of the arc mode.

The cells used in this study are murine colon cancer cells attached in a 2D environment to the bottom of a plastic well plate. First of all for future experiments, it would be useful to work with a human cancer cell line and a primary cell line as a control for non-cancer cells, as the J-plasma is believed to selectively cause more damage in cancer cell lines than in non-cancer cells. Moreover, these 2D cell models are not very representative of what happens in the human body. Therefore, it would be beneficial to work with spheroids in the future. Spheroids are multicellular 3D aggregates of cells with an O_2/CO_2, nutrient and waste gradient that create in vivo-like behaviour. These cell models can be obtained homocellularly and at low cost and provide a reliable representation of what happens in the human body. In addition, cuboids can also be used. These are micro dissected tissues with well-preserved tissue microenvironments, which means they could be used as an even better representation of a peritoneal metastasis.

4.3.2 Suggestions for future work

Building on this study, first of all, flow cytometry can also be performed on the cells of the plastic well plate immediately after treatment. Thus, information regarding direct cell death in plastic could also be obtained and compared with the aluminium results. Conversely, an MTS assay could be carried out on the cells from aluminium to determine indirect cell death, but one would have to wait 48-72 h after treatment before performing this experiment. Since it is assumed that the cells cannot adhere to aluminium, they would have to be transferred to plastic falcons during this waiting period to continue their growth undisturbed. This process then again creates doubt regarding the relevance for a medical setting.

Second, analyses can be performed using the IncuCyte ZOOM device. This is a live cell imaging and analysis platform that allows automatic quantification of cell behaviour over time. The system enables time-based curves of cellular activities such as 2D and 3D growth, migration, aggregation and invasion. Moreover, fluorescence tracing enables phagocytosis testing, cell viability monitoring and apoptosis. A major advantage is the kinetic information that is impossible to obtain with MTS assay or flow cytometry.

Third, future research is needed to better understand the mechanisms of cell death by CAP. Currently, the main theory is cell death by generation of reactive species. To better understand

this, research could be done on the chemistry of the liquid phase. By doing so, the reactive species can be identified and the possible link with cell death can be investigated.

Overall, there is a wide variety of devices that work with different methods, e.g. specific gas flows, to generate CAP. This means that it is difficult to compare devices and their respective investigations. Therefore, it could be useful for future research to provide a standardised setup that can be applied to the different devices. This includes the set distances, power, different gases with gas flow and exposure times. Then, in vivo studies should be carried out to investigate the benefits for patients, such as additional life years and improvement in quality of life, in addition to potential hazards and side effects. Finally, it might be beneficial to conduct the experiments on a larger scale to have a better statistical basis. This should also help reduce bias due to human error, as many of the operations were performed by hand.

In general, much is still unknown about the mechanism of action of CAP. Therefore, the findings in this study are mainly based on assumptions and hypotheses from previous studies. Future research could provide more certainty in confirming some of these hypotheses.

5. Conclusion

The results of this experimental setup showed that CAP caused direct immediate cell death and indirect delayed cell death in murine colon cancer cells after irradiation at 10 mm distance above the medium surface at 8 W or 16 W for 30 s or 120 s of treatment. According to the results, a 120-second treatment almost always caused more cell death than a 30-second treatment. Further research could reveal whether this is a general trend or rather a chance finding. Since the experiments were performed in aluminium or plastic well plates and the murine cancer cells were treated while in medium, it is not known whether these results can be extrapolated to human cancer cell lines. The exact mechanism behind the observed cell death by CAP remains unknown. To better understand this, future experiments could be conducted that also more closely resemble the human conditions.

6. References

1. Sung H, Ferlay J, Siegel RL, Laversanne M, Soerjomataram I, Jemal A, et al. Global Cancer Statistics 2020: GLOBOCAN Estimates of Incidence and Mortality Worldwide for 36 Cancers in 185 Countries. CA Cancer J Clin. 2021;71(3):209-49.
2. Ljubičić N, Poropat G, Antoljak N, Bašić Marković N, Amerl Šakić V, Rađa M, et al. OPPORTUNISTIC SCREENING FOR COLORECTAL CANCER IN HIGH-RISK PATIENTS IN FAMILY MEDICINE PRACTICES IN THE REPUBLIC OF CROATIA. Acta Clin Croat. 2021;60(Suppl 2):17-26.
3. register Bc. Cijfers over kanker. Belgian cancer register.
4. Dekker E, Tanis PJ, Vleugels JLA, Kasi PM, Wallace MB. Colorectal cancer. Lancet. 2019;394(10207):1467-80.
5. Loupakis F. The importance of exposing patients with metastatic colorectal cancer to all treatment options. Clin Adv Hematol Oncol. 2021;19 Suppl 3(1):3-5.
6. Biller LH, Schrag D. Diagnosis and Treatment of Metastatic Colorectal Cancer: A Review. Jama. 2021;325(7):669-85.
7. Ceelen WP, Bracke ME. Peritoneal minimal residual disease in colorectal cancer: mechanisms, prevention, and treatment. Lancet Oncol. 2009;10(1):72-9.
8. Gremonprez F, Willaert W, Ceelen W. Animal models of colorectal peritoneal metastasis. Pleura Peritoneum. 2016;1(1):23-43.
9. Schneider C, Arndt S, Zimmermann JL, Li Y, Karrer S, Bosserhoff AK. Cold atmospheric plasma treatment inhibits growth in colorectal cancer cells. Biol Chem. 2018;400(1):111-22.
10. Yan D, Xu W, Yao X, Lin L, Sherman JH, Keidar M. The Cell Activation Phenomena in the Cold Atmospheric Plasma Cancer Treatment. Sci Rep. 2018;8(1):15418.
11. Ahn HJ, Kim KI, Kim G, Moon E, Yang SS, Lee JS. Atmospheric-pressure plasma jet induces apoptosis involving mitochondria via generation of free radicals. PLoS One. 2011;6(11):e28154.
12. Faramarzi F, Zafari P, Alimohammadi M, Moonesi M, Rafiei A, Bekeschus S. Cold Physical Plasma in Cancer Therapy: Mechanisms, Signaling, and Immunity. Oxid Med Cell Longev. 2021;2021:9916796.
13. Yan X, Xiong ZL, Zou F, Zhao SS, Lu XP, Yang GX, et al. Plasma-Induced Death of HepG2 Cancer Cells: Intracellular Effects of Reactive Species. Plasma Processes and Polymers. 2012;9(1):59-66.
14. Yan DY, Malyavko A, Wang QH, Lin L, Sherman JH, Keidar M. Cold Atmospheric Plasma Cancer Treatment, a Critical Review. Applied Sciences-Basel. 2021;11(16).

15. Fridman G, Friedman G, Gutsol A, Shekhter AB, Vasilets VN, Fridman A. Applied plasma medicine. Plasma Processes and Polymers. 2008;5(6):503-33.
16. Dubuc A, Monsarrat P, Virard F, Merbahi N, Sarrette JP, Laurencin-Dalicieux S, et al. Use of cold-atmospheric plasma in oncology: a concise systematic review. Ther Adv Med Oncol. 2018;10:1758835918786475.
17. Partecke LI, Evert K, Haugk J, Doering F, Normann L, Diedrich S, et al. Tissue tolerable plasma (TTP) induces apoptosis in pancreatic cancer cells in vitro and in vivo. BMC Cancer. 2012;12:473.
18. Tendero C, Tixier C, Tristant P, Desmaison J, Leprince P. Atmospheric pressure plasmas: A review. Spectrochimica Acta Part B-Atomic Spectroscopy. 2006;61(1):2-30.
19. Keidar M, Walk R, Shashurin A, Srinivasan P, Sandler A, Dasgupta S, et al. Cold plasma selectivity and the possibility of a paradigm shift in cancer therapy. Br J Cancer. 2011;105(9):1295-301.
20. Köritzer J, Boxhammer V, Schäfer A, Shimizu T, Klämpfl TG, Li YF, et al. Restoration of sensitivity in chemo-resistant glioma cells by cold atmospheric plasma. PLoS One. 2013;8(5):e64498.
21. Lin A, Gorbanev Y, De Backer J, Van Loenhout J, Van Boxem W, Lemière F, et al. Non-Thermal Plasma as a Unique Delivery System of Short-Lived Reactive Oxygen and Nitrogen Species for Immunogenic Cell Death in Melanoma Cells. Adv Sci (Weinh). 2019;6(6):1802062.
22. Keidar M, Yan D, Sherman JH. Cold plasma cancer therapy. California, CA, USA: Morgan & Claypool 2019.
23. Fridman A, Chirokov A, Gutsol A. Non-thermal atmospheric pressure discharges. Journal of Physics D-Applied Physics. 2005;38(2):R1-R24.
24. Hong Y, Lu N, Pan J, Li J, Wu Y, Shang KF. Electrical and Spectral Characteristics of a Low-Temperature Argon-Oxygen Plasma Jet With Syringe Needle-Ring Electrodes. Ieee Transactions on Plasma Science. 2013;41(3):545-52.
25. Weltmann KD, Kindel E, Brandenburg R, Meyer C, Bussiahn R, Wilke C, et al. Atmospheric Pressure Plasma Jet for Medical Therapy: Plasma Parameters and Risk Estimation. Contributions to Plasma Physics. 2009;49(9):631-40.
26. Waskoenig J, Niemi K, Knake N, Graham LM, Reuter S, Schulz-von der Gathen V, et al. Diagnostic-based modeling on a micro-scale atmospheric-pressure plasma jet. Pure and Applied Chemistry. 2010;82(6):1209-22.
27. Barekzi N, Laroussi M, Konesky G, Roman S. Effects of low temperature plasma on prostate cancer cells using the Bovie Medical J-Plasma (R) device. Plasma Processes and Polymers. 2016;13(12):1189-94.

28. Mahdikia H, Saadati F, Freund E, Gaipl US, Majidzadeh AK, Shokri B, et al. Gas plasma irradiation of breast cancers promotes immunogenicity, tumor reduction, and an abscopal effect in vivo. Oncoimmunology. 2020;10(1):1859731.
29. Kim CH, Bahn JH, Lee SH, Kim GY, Jun SI, Lee K, et al. Induction of cell growth arrest by atmospheric non-thermal plasma in colorectal cancer cells. J Biotechnol. 2010;150(4):530-8.
30. Szili EJ, Hong SH, Oh JS, Gaur N, Short RD. Tracking the Penetration of Plasma Reactive Species in Tissue Models. Trends Biotechnol. 2018;36(6):594-602.
31. Hasse S, Meder T, Freund E, von Woedtke T, Bekeschus S. Plasma Treatment Limits Human Melanoma Spheroid Growth and Metastasis Independent of the Ambient Gas Composition. Cancers (Basel). 2020;12(9).
32. Fantz U. Basics of plasma spectroscopy. Plasma Sources Science & Technology. 2006;15(4):S137-S47.
33. Terry L Riss RAM, Andrew L Niles, Sarah Duellman, Hélène A Benink, Tracy J Worzella and Lisa Minor. Cytotoxicity Assays: In Vitro Methods to Measure Dead Cells: Eli Lilly & Company and the National Center for Advancing Translational Sciences; 2019.
34. Jahan-Tigh RR, Ryan C, Obermoser G, Schwarzenberger K. Flow cytometry. J Invest Dermatol. 2012;132(10):1-6.

7. Supplementary data

7.1 Gating strategy

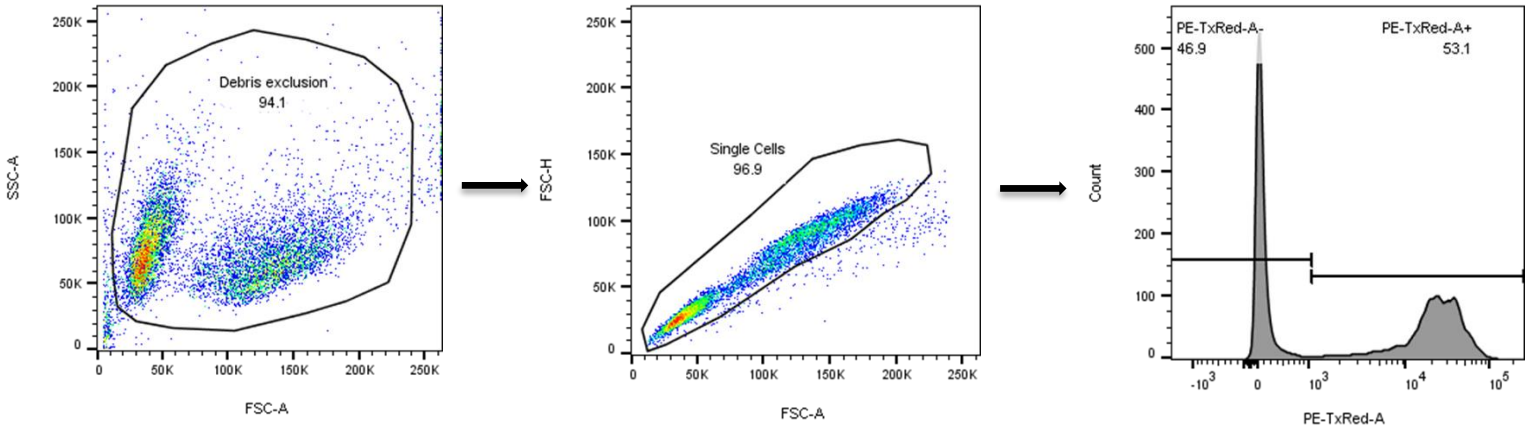

Figure S1: Gating strategy example of MC38 – Sample A4. *In the first image the debris, caused by cell death, is excluded from the cell population. Next single cells are selected, followed by the division into dead and live cells.*

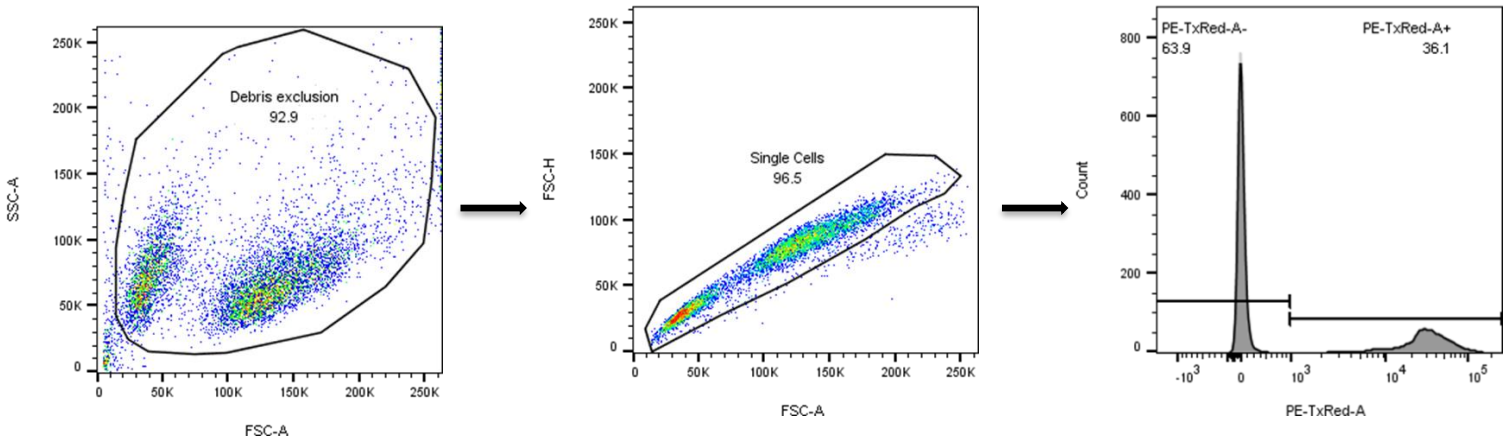

Figure S2: Gating strategy example of CT26 – Sample A4. *In the first image the debris, caused by cell death, is excluded from the cell population. Next single cells are selected, followed by the division into dead and live cells.*

7.2 Cell counts flow cytometry

Table S1: Amount of counts in flow cytometry per well, divided by live cells (A-) and death cells (A+). *Treatment condition A1 = B1 = C1 = 10 mm, 8 W, 30 s, A2 = B2 = C2 = 10 mm, 8 W, 120 s, A3 = B3 = C3 = 10 mm, 16 W, 30 s, A4 = B4 = C4 = 10 mm, 16 W, 120 s, A5 = B5 = C5 = control*

Sample:	Debris exclusion/Single Cells/PE-TxRed-A+ | Count	Debris exclusion/Single Cells/PE-TxRed-A- | Count	Total Counts
CT26_A1	1043	5724	7914
CT26_A2	1630	4866	7416
CT26_A3	931	3399	5080
CT26_A4	2650	4683	8179
CT26_A5	236	2931	4326
CT26_B1	1368	7178	9854
CT26_B2	2332	5928	9448
CT26_B3	1139	4625	6554
CT26_B4	1516	4565	6827
CT26_B5	582	3690	5604
CT26_C1	1135	4698	6856
CT26_C2	1855	3527	6244
CT26_C3	1276	4140	6134
CT26_C4	4017	4830	10000
CT26_C5	517	3250	5111
MC38_A1	2205	6024	10000
MC38_A2	5408	3330	10000
MC38_A3	2556	6357	10000
MC38_A4	4840	4276	10000
MC38_A5	562	4209	6947
MC38_B1	2411	6487	10000
MC38_B2	3103	1911	5768
MC38_B3	2216	6685	10000
MC38_B4	2521	6318	10000
MC38_B5	259	6807	8567

MC38_C1	3015	6127	10000
MC38_C2	2373	1646	4606
MC38_C3	1632	3268	5696
MC38_C4	2859	5025	8563
MC38_C5	259	8163	10000

7.3 Statistical analysis

Tests of Homogeneity of Variances

		Levene Statistic	df1	df2	Sig.
Debris exclusion/Single Cells/PE-TxRed-A+ | Freq. of Parent	Based on Mean	2,024	4	10	,167
	Based on Median	1,262	4	10	,347
	Based on Median and with adjusted df	1,262	4	5,099	,392
	Based on trimmed mean	1,979	4	10	,174

ANOVA

Debris exclusion/Single Cells/PE-TxRed-A+ | Freq. of Parent

	Sum of Squares	df	Mean Square	F	Sig.
Between Groups	1089,890	4	272,473	9,104	,002
Within Groups	299,298	10	29,930		
Total	1389,188	14			

Figure S3: One-way ANOVA on flow cytometry results from CT26 cells in SPSS.

Tests of Homogeneity of Variances

		Levene Statistic	df1	df2	Sig.
Debris exclusion/Single Cells/PE-TxRed-A+ | Freq. of Parent	Based on Mean	3,449	4	10	,051
	Based on Median	1,058	4	10	,426
	Based on Median and with adjusted df	1,058	4	4,422	,472
	Based on trimmed mean	3,216	4	10	,061

ANOVA

Debris exclusion/Single Cells/PE-TxRed-A+ | Freq. of Parent

	Sum of Squares	df	Mean Square	F	Sig.
Between Groups	4714,637	4	1178,659	27,474	<,001
Within Groups	429,014	10	42,901		
Total	5143,652	14			

Figure S4: One-way ANOVA on flow cytometry results from MC38 cells in SPSS.